Reaction Behavior of the Li-N-H Hydrogen Storage System with Boron Nitride as an Additive

LINNAN DU, GEORG MAUER, and ROBERT VAßEN

This work begins with a discussion of the desorption, reaction rate-limiting step of a $LiNH_2$-LiH hydrogen storage system. Using microstructural and thermodynamic studies, it explains the working mechanism of BN as an additive in Li-N-H hydrogen storage materials. High-energy wet ball milling with THF was applied to the $LiNH_2$ + $1.2LiH$ mixture. The results obtained in this work show that the rate-limiting step of the desorption reaction depends on the degree of oxidation and amount of LiH in the system. The activation energy of the desorption reaction of both ball-milled $LiNH_2$ and $LiNH_2$ + $1.2LiH$ samples was reduced with BN as an additive. BN had no clear impact on the crystallite sizes of $LiNH_2$ + $1.2LiH$ as-milled samples. However, it was found that BN stabilizes the crystallite sizes of $LiNH_2$ + $1.2LiH$ samples during the high-temperature desorption and absorption processes.

I. INTRODUCTION

As a clean energy carrier, hydrogen has attracted great attention. It is carbon-free, abundantly available from water, and has an exceptional gravimetric energy density which can reach up to 142 MJ/kg.[1] However, the problem with hydrogen energy is that it exists as a low-density gas at atmospheric pressure and room temperature. Therefore, suitable solid-state hydrogen storage materials with high storage capacities are an important issue for the hydrogen energy economy.

The US Department of Energy (DOE) has defined standards for an on-board hydrogen storage system. The target for the year 2010[2,3] was a system storage capacity exceeding 6 wt pct (2.0 kWh/kg) at around 373 K (100 °C).[4] However, at the time of writing, a new target had been set[2] for the year 2017, namely 5.5 wt pct (1.8 kWh/kg). Due to the high theoretical storage capacity, many metal hydrides and complex hydrides have shown significant potential for use as reversible, solid, hydrogen storage materials. Of the complex hydride hydrogen storage materials, the $LiNH_2$ + LiH system has a relatively high theoretical storage capacity (>6 wt pct) and a relatively low desorption temperature [<523 K (250 °C)]. In contrast to other metal hydrides or complex hydrides, the Li-N-H system is composed of both metallic and non-metallic elements in which the storage process involves the breaking and forming of non-metal hydrogen bonds.[5] Chen et al.[6] were the first to describe the Li-N-H hydrogen storage system:

$$LiNH_2 + LiH \leftrightarrow Li_2NH + H_2 \quad [1]$$

Many studies have investigated the reaction mechanism of Reaction [1].[7,8] First reported by Hu and Ruckenstein[9] and Ichikawa et al.,[10] it is now well accepted that the reaction shown in (1) can be further separated into two reaction steps:[11–15]

$$2LiNH_2 \rightarrow Li_2NH + NH_3 \quad [2]$$

$$NH_3 + LiH \rightarrow LiNH_2 + H_2 \quad [3]$$
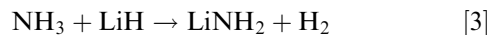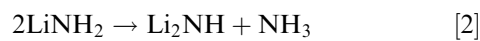
$LiNH_2$ first decomposes into Li_2NH and releases NH_3; then NH_3 reacts with LiH and H_2 is released. The product $LiNH_2$ decomposes and releases NH_3 again, and this NH_3 reacts with LiH further until all remaining $LiNH_2$ and LiH transform into Li_2NH and H_2.[7]

Despite its hydrogen capacity, the system is restricted by low reaction kinetics.[16] As the thermodynamic properties of the Li-N-H system are thought to be poor,[17] several scientists have tried to introduce Mg as an element or to use MgH_2 instead of LiH together with $LiNH_2$.[18–22] However, thermodynamically accurate results are still not available, because the kinetic properties are significantly worse.[23] Besides lab work, some scientists also focused on identifying $LiNH_2$ + LiH hydrogen storage system with first-principles calculation methods.[5,24,25]

Several papers[7,9,14,26] report that the reaction rate of Reaction [3] is very fast. However, Yao suggested that the rate-limiting step should be Reaction [3].[12] Using Mn and V as additives, Yao and co-workers successfully enhanced the release of NH_3 from $LiNH_2$, but this had little influence on the production of H_2.[12] Varin[13] assumed that LiH partially reacts with residual oxygen and water vapor, forming LiOH, and that it thus becomes inactive for Reaction [3], which is a major

LINNAN DU, Scientific Assistant, GEORG MAUER, Head of Research Team, and ROBERT VAßEN, Head of Department, are with the Forschungszentrum Jülich GmbH, IEK-1, 52425 Jülich, Germany. Contact e-mail: g.mauer@fz-juelich.de

impediment to hydrogen desorption. They suggested using a little more LiH with a molecular ratio of $LiNH_2$ to LiH of 1:1.2. With regard to another aspect, Pinkerton found that the reaction rate was dependent on the sample amount. Larger sample sizes are more likely to develop local NH_3 concentrations which are high enough to inhibit further reaction.[27] He believed that the activation energy for the decomposition reaction was independent of the milling time. However, Shaw et al. came to a different conclusion.[28] Obviously, there is still no consensus about the reaction mechanism and the rate-limiting step. For this reason, the present work will firstly focus on clarifying the desorption mechanisms. The desorption experiments with $LiNH_2$ samples are performed in both gravimetric and volumetric systems at the same desorption temperature. The results are then compared and analyzed.

In order to improve the desorption properties, several additives have been used with the Li-N-H system, for example Ti (nanoparticles), Ti (microparticles), TiO_2 (nanoparticles), TiO_2 (microparticles),[29] $TiCl_3$,[29–32] Mn, V,[12] etc. Recently, Dong et al. showed that KBr, KCl, KF, and KOH effectively enhance the reaction kinetics between LiH and NH_3.[33] Compared with other additives, nitrides were then proposed as a new group of additives. BN was reported to improve the dehydrogenation rate of the Li-N-H system[16] and improve Li + diffusion between $LiNH_2$ and LiH.[8] High-energy dry ball milling[10,12,28] and hollow nanosphere structures[34] have also been used to enhance the kinetics of reaction. In our previous work, we also found that 3 wt pct BN successfully improved the recyclability of the $LiNH_2$ + LiH system.[35] However, the detailed mechanism is still unclear. Thus, this work also aims to detail the hydrogen storage ability of the $LiNH_2$ + 1.2LiH system with and without BN as an additive. The changes in desorption activation energies, enthalpies, and crystallite sizes were studied and compared during desorption of the $LiNH_2$ + 1.2LiH wet ball-milled samples with and without BN.

II. EXPERIMENTAL METHODS

Lithium amide ($LiNH_2$, purity 95 pct) and lithium hydride (LiH, purity 98 pct) were purchased as powders from Sigma-Aldrich Chemie GmbH. Tetrahydrofuran (THF, purity 99.5 pct) was supplied by Acros Organics. The additive (BN, purity 98 pct) was purchased from Sigma-Aldrich Chemie GmbH. All samples were stored and handled in a glove box under a protective argon atmosphere. The molecular ratio between $LiNH_2$ and LiH was set to 1:1.2, as suggested in Reference 13. The planetary ball milling method was applied in this study using planetary mills PM 400 (RETSCH GMBH, Germany). Similar to References 35,36, the samples in the present work were wet ball milled with THF. Yttria-stabilized zirconia (YSZ) milling balls (Tosoh Corporation, Japan) were used as milling media. The weight ratio between THF and the sample material was 4:1. This resulted in a mixture of 20 g THF and 50 g milling balls per 5 g sample powder. Samples in this study were milled with a mixture of milling balls with different diameters. The weight ratio between 5 mm milling balls and 2 mm milling balls was 7:3. The milling time was 72 hours. After milling, the wet ball-milled suspensions were stored in the glove box for about 20 hours in order to evaporate the THF.

Desorption measurements of the wet ball-milled $LiNH_2$ samples were processed first in the volumetric apparatus BELSORP-HP (BEL Japan, Osaka, Japan) and in the gravimetric system IsoSORP-Hygra (RU-BOTHERM GmbH, Bochum, Germany) at 573 K (300 °C). As the BELSORP-HP system is a closed volume system, the pressure change during the sorption experiment can be measured and recorded. The weight changes of the samples during the sorption process are calculated based on the pressure change. The ISOSORP-Hygra comprises a magnetic suspension balance. During the experiment, the pressure can be kept at a specified value (in this work it was kept as vacuum), and the weight change of the sample can be read directly.

In order to study the BN influence on the desorption enthalpy of the $LiNH_2$ + 1.2 LiH samples, hydrogen desorption measurements of the wet ball-milled samples with and without BN were processed in the volumetric apparatus BELSORP-HP. Samples were desorbed at 4 different temperatures in the range from 523 K to 598 K (250 °C to 325 °C). The desorption time was 3 hours in each case. Based on the different equilibrium pressures arising at the different temperatures in the Belsorp-HP system, the enthalpy change of the desorption was calculated using the Van't Hoff equation.

About 60–70 mg of $LiNH_2$ and $LiNH_2$ + 1.2LiH ball-milled samples with and without BN was also studied with DTA/TG methods (STA449C Jupiter, Netzsch). The samples were heated from 323 K to 673 K (50 °C to 400 °C) or 573 K (300 °C) at heating rates of 1, 2, and 5 K/minute with Ar as the desorption atmosphere, respectively. Based on the DTA profile, the activation energies of Reactions [1] and [2] were calculated by means of the Kissinger method.[37]

The phase compositions of the $LiNH_2$ + 1.2LiH as-milled samples and the samples after sorption were analyzed by X-ray diffraction (XRD) with a Bruker D4 ENDEAVOUR diffractometer (Bruker AXS GmbH, Karlsruhe). The wet ball-milled $LiNH_2$ + 1.2LiH samples with and without BN were desorbed at 523 K (250 °C). After this, absorption experiments were performed with some of these samples. The absorption temperature was 473 K (200 °C) with an initial absorption pressure of approx. 1000 kPa. The desorption and absorption time for each sample was 3 hours, respectively. Based on the XRD information, the crystallite sizes of the samples were determined by applying the Williamson–Hall method.[38]

III. RESULTS

A. Desorption Analysis of LiNH_2 Samples

1. BN influence on the desorption of $LiNH_2$
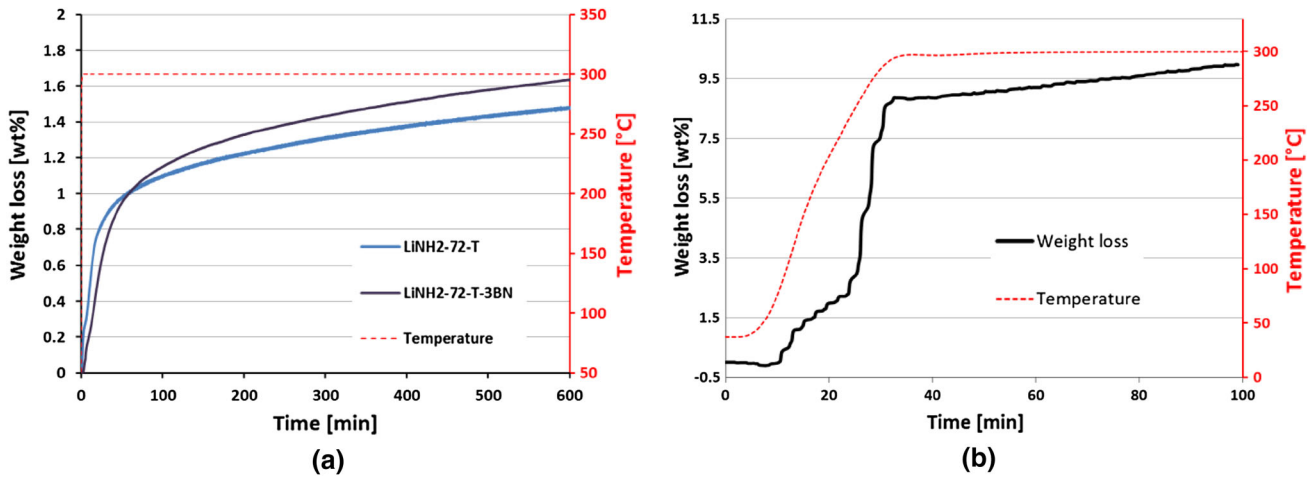Figure 1(a) illustrates the slow hydrogen desorption kinetics for both of the $LiNH_2$ samples with and without

Fig. 1—(a) LiNH$_2$ samples (with and without BN): desorption profile at 573 K (300 °C) in the volumetric Belsorp-HP system; (b) LINH$_2$ sample with BN (LiNH$_2$-72-T): desorption profile at 573 K (300 °C) in the gravimetric magnetic suspension balance system; the dashed red lines indicate the temperature profile (Color figure online).
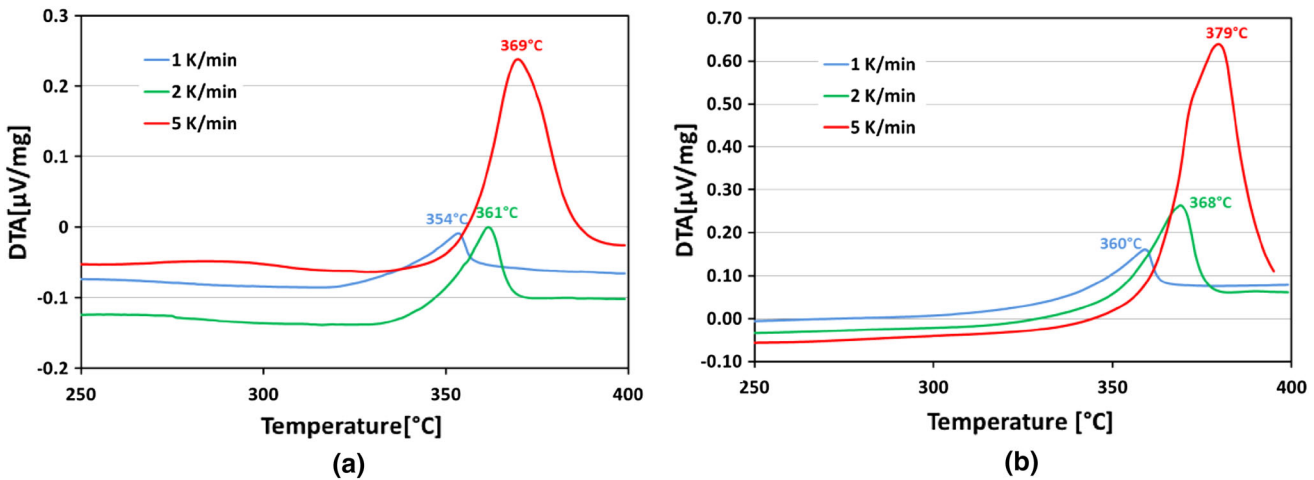

Fig. 2—DTA results of (a) LiNH$_2$: 72 h wet ball milled; (b) LiNH$_2$ + 3 wt pct BN: 72 h wet ball milled; heating rate 1, 2, and 5 K/min, experiment atmosphere: Ar.

BN, respectively, desorbed at 573 K (300 °C) with the volumetric Belsorp-HP system. The maximum weight loss of LiNH$_2$ is theoretically 36.9 pct. With this volumetric system, only around 1.4–1.7 wt pct weight loss was achieved within 550 minute. Figure 1(b) shows the desorption profile of a 61 mg LiNH$_2$ sample (without BN) at 573 K (300 °C) with the gravimetric (IsoSORP-MSB) system. During the heating process, the pressure of the system was kept at vacuum level. It is obvious that the weight loss measured with the IsoSORP-MSB system had already reached 10 pct within 100 min. After a temperature of 573 K (300 °C) was reached, the weight loss rate tended to be constant. The desorption rate was much higher than the result obtained with the Belsorp-HP system.

2. *BN influence on the desorption activation energy of LiNH$_2$ samples*

DTA analyses were performed with LiNH$_2$ samples. All DTA experiments with the LiNH$_2$ samples revealed

one prominent endothermic peak in the temperature range between 623 K and 673 K (350 °C and 400 °C) (see Figure 2), which is in agreement with the published data from Varin and Yang.[11] Based on the peak temperatures and heating rates, the activation energies of the samples were calculated using the Kissinger method. The corresponding linear fits are shown in Figure 3. The resulting activation energies were 321.8 ± 33.2 kJ/mol NH$_3$ and 260.2 ± 18.0 kJ/mol NH$_3$, respectively. Both R^2 values (the square of the linear regression coefficient) were better than 0.95. The results suggest that the addition of BN can lower the activation energy of the LiNH$_2$ decomposition reaction.

B. *Study of LiNH$_2$ + 1.2LiH Samples*

1. *BN influence on the desorption enthalpy of LiNH$_2$ + 1.2LiH samples*

In order to study the BN influence on the desorption enthalpy of the samples, the desorption results are

illustrated in Figure 4. The higher the desorption temperature, the faster the initial desorption kinetics and the higher the final pressure, which was reached after approx. 60 minute.

Applying the Van't Hoff equation, the enthalpy can be derived from a plot of $\ln(P/P_0)$ vs $1000/T$. For each sample, there were 4 data points at 4 different temperatures. Figure 5 illustrates the linear fits. From the slopes of the regression lines, the desorption enthalpies and entropies were calculated and are given in the figures. The R^2 values were larger than 0.93.

Considering the margin of error, there are no significant differences between samples with and without BN (33 ± 4 and 30 ± 4 kJ/mol). The results clearly illustrate that BN has no influence as an additive on the desorption enthalpy.

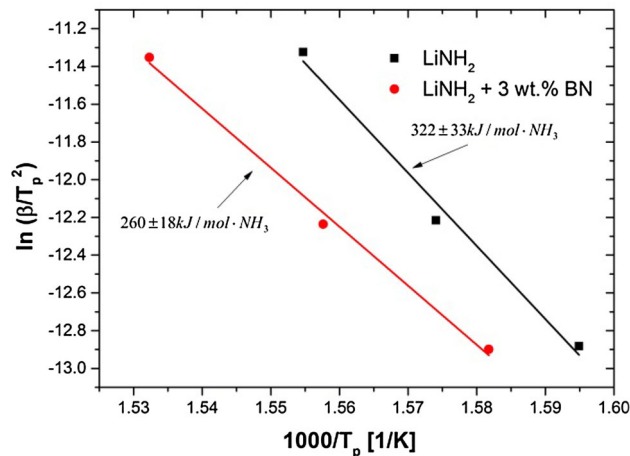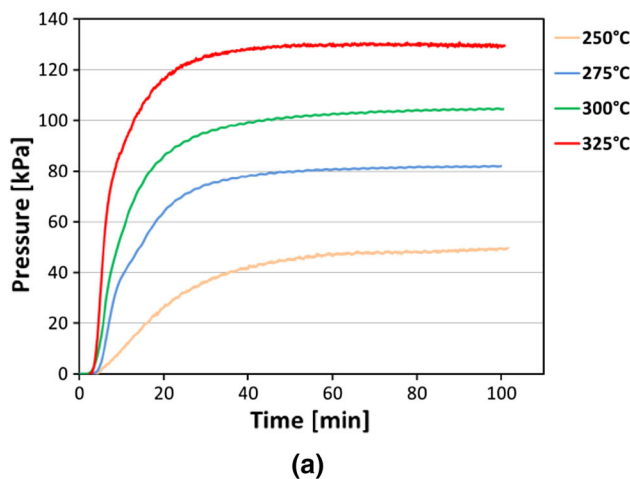Chen et al.[6] reported a desorption enthalpy of 45 kJ/mol. Varin and Yang[11] published an enthalpy of 62.4 kJ/mol for the material system without an additive. Although slightly lower, the results of this study are in reasonable accordance with their work.

2. *BN influence on the desorption activation energy of LiNH₂ + 1.2LiH samples*

Similar to LiNH₂ single-component samples, the LiNH₂ + 1.2LiH samples were studied using the DTA method. The results are shown in Figure 6.

Similar to the findings of Yao et al.[12] and Varin et al.,[13] the weight losses of the samples were accompanied by a very broad endothermic DTA peak. In order to calculate the activation energy, the peak point (T_p) of the DTA result was determined. For each sample material, the 3 heating rates yielded 3 DTA peaks. A linear regression of $\ln(\beta/T_p^2)$ (β being the heating rate) as a function of $1000/T_p$ yielded the lines in Figure 7. The corresponding R-square values were larger than 0.95. Applying the Kissinger method, the activation energy E_a can be calculated from the slope of the linear fit curves in Figure 7. For the sample without additives, E_a was calculated as 84.7 ± 12.0 kJ/mol, which is very close to the published data (85 kJ/mol) for the same system.[11] For the sample with 3 wt pct BN, a significantly lower activation energy E_a of 68.0 ± 6.5 kJ/mol was calculated.

3. *BN influence on the crystallite sizes of LiNH₂ + 1.2LiH samples after desorption/absorption cycles*

The XRD patterns of the samples as-milled and after desorption and absorption are shown in Figure 8. From the results, it can be seen that for the as-milled samples and the samples after absorption, the main phases are LiNH₂ and LiH. For the samples after desorption, the main phase is Li₂NH. Obviously, the existence of BN does not significantly affect the phase change of the sample during milling and sorption processes.

Based on the XRD pattern data, the crystallite sizes of the milled samples and the samples after desorption/absorption were calculated by applying the Williamson-Hall method. The calculation results are shown in Figure 9.
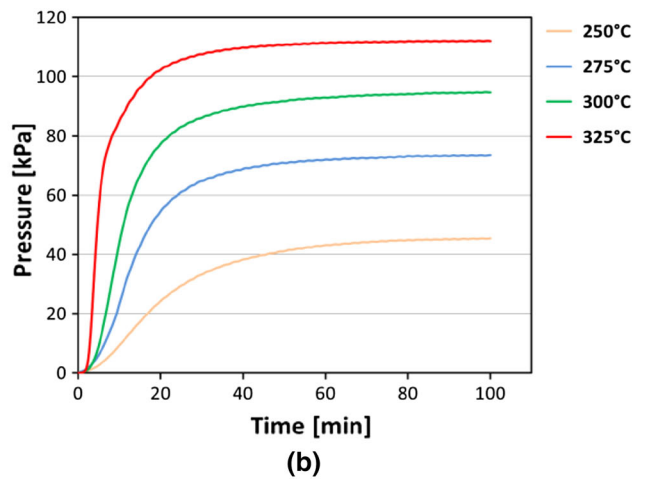

Fig. 3—Based on the DTA data in Fig. 2, the activation energy was calculated for LiNH₂ samples with and without BN using the Kissinger method.

(a)

(b)

Fig. 4—Desorption profiles of samples in the volumetric Belsorp-HP system. (*a*) LiNH₂ + 1.2LiH; (*b*) LiNH₂ + 1.2LiH + 3 wt pct BN; desorption temperatures were 523 K, 548 K, 573 K, and 598 K (250 °C, 275 °C, 300 °C, and 325 °C).

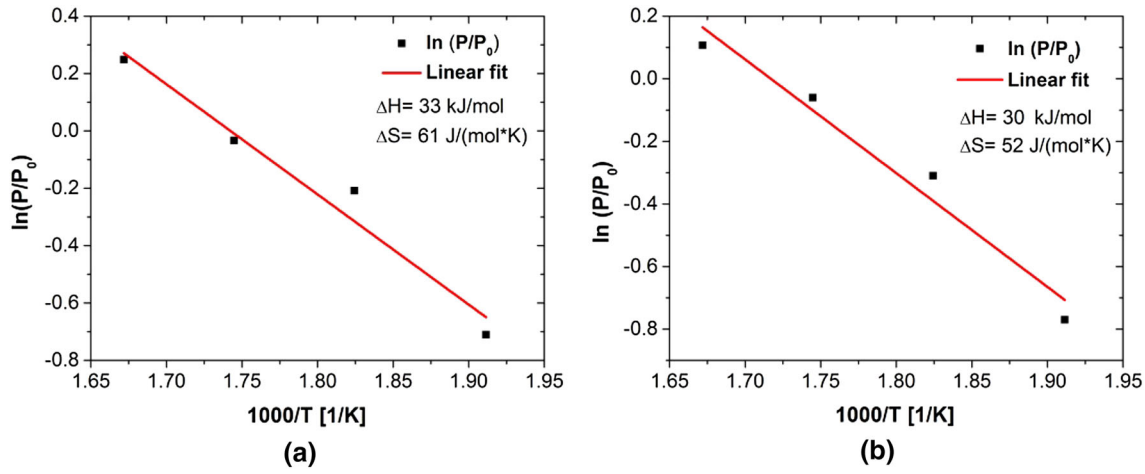Fig. 5—Based on the result in Fig. 4, the enthalpy was calculated for the samples (*a*) LiNH$_2$ + 1.2LiH and (*b*) LiNH$_2$ + 1.2LiH + 3 wt pct BN using the Van't Hoff equation.
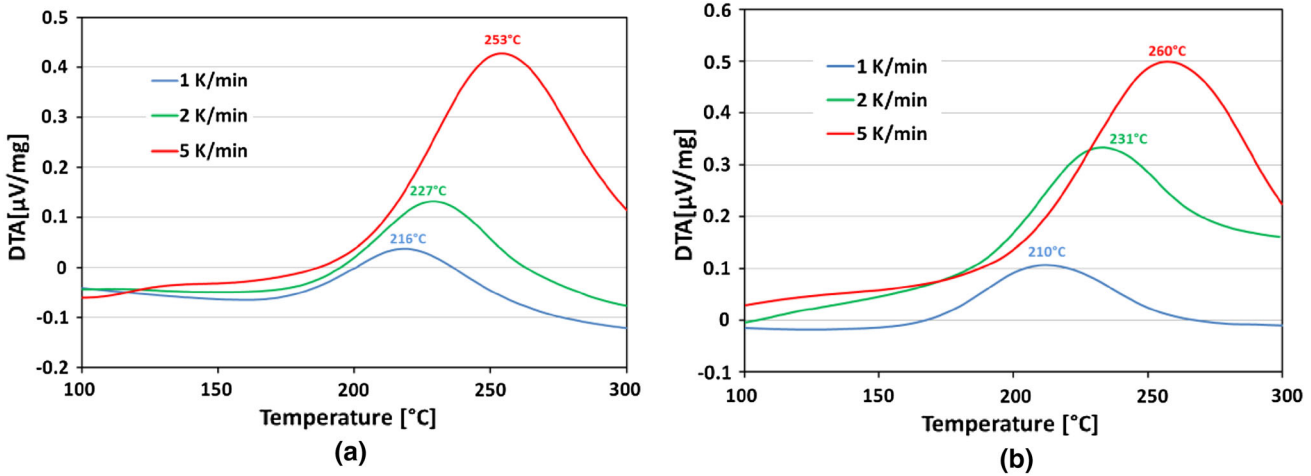
Fig. 6—DTA results of (*a*) LiNH$_2$ + 1.2LiH and (*b*) LiNH$_2$ + 1.2LiH + 3 wt pct BN samples; heating rates: 1, 2, and 5 K/min, experiment atmosphere: Ar.
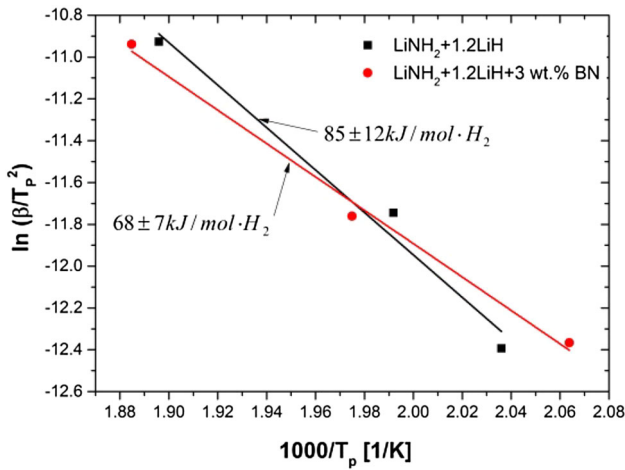

Fig. 7—Based on the result in Fig. 6, the activation energy was calculated for sample LiNH$_2$ + 1.2LiH with and without BN using the Kissinger method.

As shown in Figure 9, the crystallite size of the sample without BN increased after the 3-hour desorption. After the subsequent absorption, the crystallite size reached almost twice the size of the as-milled original. In contrast, after the same cycle of 3 hours of desorption and absorption, the sample with 3 wt pct BN showed no significant change in crystallite size, as can be seen in Figure 9. This might be an indication that BN efficiently stabilizes the crystallite size of the LiNH$_2$ + 1.2LiH system during hydrogen sorption processes.

IV. DISCUSSION

A. *Reaction Process Analysis of Pure LiNH$_2$*

In the former work, we found that BN as an additive clearly improves the recyclability of the LiNH$_2$ + 1.2 LiH hydrogen storage materials.[35] The present result in Figure 1(a) shows that the presence of 3 wt pct BN had

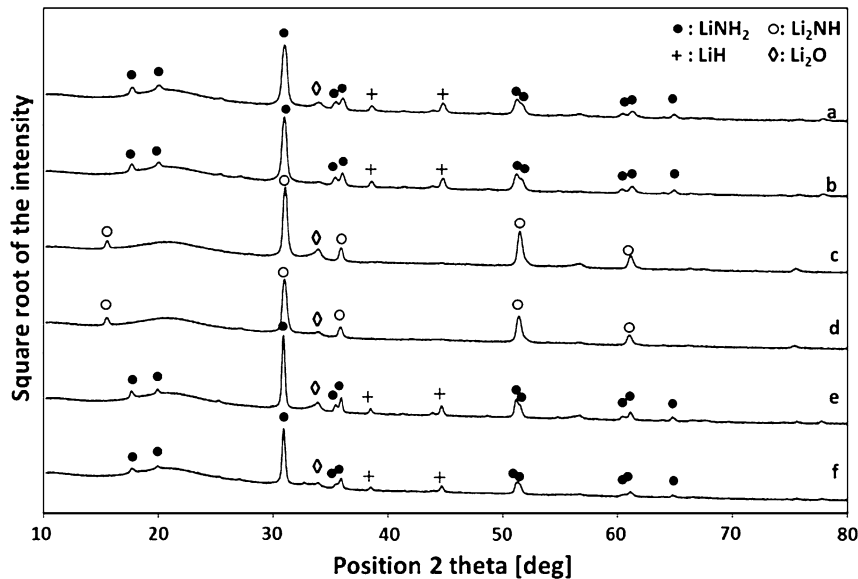Fig. 8—XRD patterns of the samples (*a*) LiNH$_2$ + 1.2LiH, 72 h wet ball milled; (*b*) LiNH$_2$ + 1.2LiH + 3 wt pct BN, 72 h wet ball milled; (*c*) LiNH$_2$ + 1.2LiH, 72 h wet ball milled, 523 K (250 °C) 3 h desorbed; (*d*)LiNH$_2$ + 1.2LiH + 3 wt pct BN, 72 h wet ball milled, 523 K (250 °C) 3 hours desorbed; (*e*) LiNH$_2$ + 1.2LiH, 72 h wet ball milled, 523 K (250 °C) desorbed, 473 K (200 °C) absorbed; LiNH$_2$ + 1.2LiH + 3 wt pct BN, 72 h wet ball milled, 523 K (250 °C) desorbed, 473 K (200 °C) absorbed.
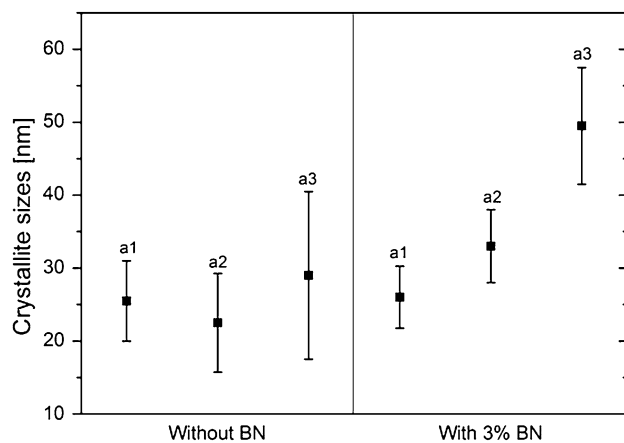

Fig. 9—Calculated LiNH$_2$ + 1.2LiH crystallite sizes of the two samples (with and without BN) after milling (a1), 523 K (250 °C), 3 h desorption (a2), and 473 K (200 °C), 3 h absorption (a3), respectively.

no influence on the desorption kinetics of the LiNH$_2$ sample, which is assumed to be the first step of the desorption process. This conclusion differs from the work of Nayebossadri *et al.*[16] which assumed that BN can effectively improve the desorption rate of the sample. On the other hand, the results in this study show that the desorbed NH$_3$ amount of LiNH$_2$ at a desorption temperature of 573 K (300 °C) differed considerably for the same period of time in the two analysis systems. The main difference between the two experimental conditions is the pressure. The higher NH$_3$ pressure suppresses the further desorption process of LiNH$_2$ very efficiently according to Eq. [2]. The low pressure in the IsoSORP-MSB system, however, supports the forward reaction of the gaseous desorption. In the vacuum condition, after the temperature reached

573 K (300 °C), the desorption rate was constant. Every mol of the LiNH$_2$ sample under study desorbed 1.70×10^{-4} mol/minute NH$_3$ at 573 K (300 °C). This result verifies that if every 1 mol of LiH could react with NH$_3$ at a rate higher than 1.70×10^{-4} mol NH$_3$/minute during the desorption process of the LiNH$_2$-LiH system, the desorption of LiNH$_2$ (which is Reaction [2]) would be the rate-limiting step. However, if every 1 mol of LiH could react with NH$_3$ at a rate lower than 1.70×10^{-4} mol NH$_3$/minute, NH$_3$ partial pressure would accumulate in the closed system. The result in Figure 1(a) shows that a low accumulated NH$_3$ partial pressure during the desorption process can stop the desorption reaction of LiNH$_2$. In this case, Eq. [3] is therefore the rate-limiting step.

B. *BN Influence on the LiNH$_2$ + 1.2LiH System*

As stated in Reference 35, the existence of BN can clearly improve the recyclability of the LiNH$_2$ + 1.2LiH samples. However, since the particle sizes of the doped and undoped LiNH$_2$ + 1.2LiH samples did not change during the desorption and absorption processes, the existence of BN obviously had no influence on the particle size. The results of the present study show furthermore that BN did not influence the desorption enthalpy of the LiNH$_2$ + 1.2LiH system either. However, the desorption activation energies of both LiNH$_2$ and LiNH$_2$ + 1.2LiH samples were reduced effectively by BN doping. This suggests that BN reduced the activation energy of the LiNH$_2$ desorption process, which is also the first step of the LiNH$_2$ + 1.2LiH desorption process, and then reduced the activation energy of the LiNH$_2$ + 1.2LiH desorption process. One possible reason for this may be that BN as a very stable phase inhibited the possible grain boundary growth during the high-energy milling process.

This effect aided material diffusion during the sorption reaction and reduced the activation energy barrier of the desorption reaction. The desorption enthalpy remained unaffected, as expected. During the desorption process, BN acted as an additive that reduced the activation energy but did not change the reaction mechanism of the sorption reaction.

The results of the XRD analyses show that BN did not alter the crystallite sizes of the $LiNH_2$ or $LiNH_2$ + 1.2LiH as-milled samples. However, BN efficiently stabilized the crystallite sizes during the sorption process. BN is a very stable phase during the sorption process. One possible reason why it stabilizes the crystallite sizes may be that the BN particles distributed throughout the samples efficiently inhibited the crystallite growth of the $LiNH_2$ + 1.2LiH samples during the sorption process. This result indicates that the decreasing kinetics of the sample without BN during the desorption cycling were due to the increase in the sample's crystallite size. By doping with BN, the crystallite size was kept small and thus a larger number of grain boundaries were achieved. This result combined with the fact that BN improved the recyclability of $LiNH_2$ + LiH samples allows us to conclude that the smaller crystallite sizes and larger grain boundaries aided the sorption processes of $LiNH_2$ + 1.2LiH hydrogen storage samples.

V. CONCLUSIONS

1. Thermodynamically, LiH is very reactive and the reaction between LiH and NH_3 is very fast. However, practically LiH is reactive and can react with residual oxygen and water vapor to form LiOH or Li_2O. This makes LiH inactive for Reaction [3], which impedes the hydrogen desorption of the $LiNH_2$-LiH system. In the study with the gravimetric system, it was shown that every 1 mol of the $LiNH_2$ sample desorbed 1.70×10^{-4} mol/minute NH_3 at 573 K (300 °C). This means that during the desorption process of the Li-N-H system, if every 1 mol of LiH (or 1.2 mol LiH in the $LiNH_2$ + 1.2 LiH system) could react with NH_3 at a rate higher than 1.70×10^{-4} mol NH_3/minute, the desorption of $LiNH_2$ (which is Reaction [2]) would be the rate-limiting step. Otherwise, NH_3 partial pressure will accumulate in the closed system and Reaction [3] will become the rate-limiting step.

2. BN as an additive efficiently decreases the desorption activation energies of the $LiNH_2$ and $LiNH_2$ + 1.2LiH samples. However, BN does not influence the desorption enthalpy of the $LiNH_2$ + 1.2LiH samples. One possible reason for this may be that the existence of BN inhibits the crystal growth during the high-energy milling process, aiding material diffusion during the sorption reaction. However, BN has no influence on the desorption reaction mechanism or on the reaction enthalpy.

3. BN has no clear influence on the crystallite sizes of either the $LiNH_2$ or $LiNH_2$ + 1.2LiH as-milled samples. However, BN efficiently stabilizes the crys-

tallite sizes during the sorption process. One possible reason may be that the distribution of BN throughout the $LiNH_2$ + 1.2 LiH samples prevents the crystallite growth of $LiNH_2$ + LiH during high-temperature desorption. This result suggests that smaller crystallite sizes and larger grain boundaries aided the sorption processes of $LiNH_2$ + 1.2 LiH samples.

REFERENCES

1. D.P. Broom: *Hydrogen Storage Materials, The Characterization of Their Storage Properties*, Springer, London, 2010, p. 5.
2. United States Department of Energy, Office of Energy Efficiency and Renewable Energy and the Freedom CAR and Fuel Partnership: "Targets for Onboard Hydrogen Storage Systems for Light-Duty Vehicles", Washington, 2009.
3. L.E. Klebanoff and J.O. Keller: *Int. J. Hydrogen Energy*, 2013, vol. 38, pp. 4533–76.
4. W. Osborn, T. Markmaitree, L.D. Shaw, J.-Z. Hu, J. Kwak, and Z. Yang: *Int. J. Hydrogen Energy*, 2009, vol. 34, pp. 4331–39.
5. G. Miceli: Dissertation, Università degli Studi di Milano-Bicocca, 2010.
6. P. Chen, Z. Xiong, J. Luo, J. Lin, and L. Tan: *Nature*, 2002, vol. 420, pp. 302–304.
7. T. Ichikawa, N. Hanada, S. Isobe, H. Leng, and H. Fujii: *J. Phys. Chem. B*, 2004, vol. 108, pp. 7887–92.
8. K.F. Aguey-Zinsou, J. Yao, and Z.X. Guo: *J. Phys. Chem. B*, 2007, vol. 111, pp. 12531–36.
9. Y.H. Hu and E. Ruckenstein: *J. Phys. Chem. A*, 2003, vol. 107, p. 9739.
10. T. Ichikawa, S. Isobe, N. Hanada, and H. Fujii: *J. Alloy Compd.*, 2004, vol. 365, pp. 271–76.
11. R.A. Varin and M. Jang: *J. Alloy Compd.*, 2001, vol. 509, pp. 7143–51.
12. J.H. Yao, C. Shang, K.F. Aguey-Zinsou, and Z.X. Guo: *J. Alloy Compd.*, 2007, vol. 432, pp. 277–82.
13. R.A. Varin, M. Jang, and M. Polanski: *J. Alloy Compd.*, 2010, vol. 491, pp. 658–67.
14. T. Markmaitree, R. Ren, and L. Shaw: *J. Phys. Chem. B*, 2006, vol. 110, pp. 20710–18.
15. J. Lu, Z. Fang, Y.J. Choi, and H.Y. Sohn: *J. Phys. Chem. C*, 2007, vol. 111, pp. 12129–34.
16. S. Nayebossadri, K.F. Aguey-Zinsou, and Z.X. Guo: *Int. J. Hydrogen Energy*, 2011, vol. 36, pp. 7920–26.
17. M. Hirscher, ed., *Handbook of Hydrogen Storage*, Wiley-VCH, Weinheim, 2010, p. 161.
18. T. Ikeda, Y. Mikami, and T. Haruki: *J. Phys. Chem. C*, 2007, vol. 111, pp. 8389–96.
19. W. Luo: *J. Alloy Compd.*, 2004, vol. 381, pp. 284–87.
20. Y. Nakamori, G. Kitahara, K. Miwa, N. Ohba, T. Noritake, S. Towata, and S. Orimo: *J. Alloy Compd.*, 2005, vols. 404–406, pp. 396–98.
21. Z. Xiong, J. Hu, G. Wu, P. Chen, W. Luo, K. Gross, and J. Wang: *J. Alloy Compd.*, 2005, vol. 398, pp. 235–39.
22. H. Leng, T. Ichikawa, S. Hino, N. Hanada, S. Isobe, and H. Fujii: *J. Phys. Chem. B*, 2004, vol. 108, pp. 8763–65.
23. M. Hirscher, ed.: *Handbook of Hydrogen Storage*, Wiley-VCH, Weinheim, 2010, pp. 162.
24. K. Miwa, N. Ohba, and S. Towata: *Phys. Rev. B*, 2005, vol. 71, p. 195109.
25. S.V. Alapati, J.K. Johnson, and D.S. Shol: *J. Phys. Chem. B*, 2006, vol. 110, pp. 8769–76.
26. L.L. Shaw, W. Osborn, T. Markmaitree, and X. Wan: *J. Power Sources*, 2008, vol. 177, pp. 500–505.
27. F.E. Pinkertion: *J. Alloy Compd.*, 2005, vol. 400, pp. 76–82.
28. L.L. Shaw, R. Ren, T. Markmaitree, and W. Osborn: *J. Alloy Compd.*, 2008, vol. 448, pp. 263–71.

29. S. Isobe, T. Ichikawa, N. Hanada, H.Y. Leng, M. Fichtner, O. Fuhr, and H. Fujii: *J. Alloy Compd.*, 2005, vols. 404–406, pp. 439–42.
30. T. Ichikawa, N. Hanada, S. Isobe, H. Leng, and H. Fujii: *Mater. Trans.*, 2005, vol. 46, pp. 1–14.
31. S. Hino, T. Ichikawa, K. Tokoyoda, Y. Kojima, and H. Fujii: *J. Alloy Compd.*, 2007, vols. 446–447, pp. 342–44.
32. T. Ichikawa, N. Hanada, S. Isobe, H.Y. Leng, and H. Fujii: *J. Alloy Compd.*, 2005, vols. 404–406, pp. 435–38.
33. B. Dong, L. Song, Y. Teng, J. Ge, and S. Zhang: *Int. J. Hydrogen Energy*, 2014, vol. xxx, pp. 1–6.
34. L. Xie, J. Zheng, Y. Liu, Y. Li, and X. Li: *Chem. Mater.*, 2008, vol. 20, pp. 282–86.
35. L. Du, G. Mauer, and R. Vaßen: *Energy Procedia*, 2012, vol. 29, pp. 147–55.
36. L. Meng: *Improved Hydrogen Sorption Kinetics in Wet Ball Milled Mg Hydrides*, 1st ed., Forschungszentrum Juelich GmbH, Juelich, 2011, p. 38.
37. H.E. Kissinger: *Anal. Chem.*, 1957, vol. 29, pp. 1702–06.
38. G.K. Williamson and W.H. Hall: *Acta Metall.*, 1953, vol. 1, pp. 22–31.